Influence of Ce–H bonding on the physical properties of the hydrides $CeCoSiH_{1.0}$ and $CeCoGeH_{1.0}$

2006 J. Phys.: Condens. Matter 18 6045

(http://iopscience.iop.org/0953-8984/18/26/022)

INSTITUTE OF PHYSICS PUBLISHING JOURNAL OF PHYSICS: CONDENSED MATTER

J. Phys.: Condens. Matter **18** (2006) 6045–6056 doi:10.1088/0953-8984/18/26/022

Influence of Ce–H bonding on the physical properties of the hydrides $CeCoSiH_{1.0}$ and $CeCoGeH_{1.0}$

B Chevalier[1,3], S F Matar[1], M Ménétrier[1], J Sanchez Marcos[2] and J Rodriguez Fernandez[2]

[1] Institut de Chimie de la Matière Condensée de Bordeaux (ICMCB), CNRS [UPR 9048], Université Bordeaux 1, Avenue du Docteur A Schweitzer, 33608 Pessac Cedex, France
[2] Departamento de Ciencias de la Tierra y Fisica de la Materia Condensada, Facultad de Ciencias, Universidad de Cantabria, 39005 Santander, Spain

E-mail: chevalie@icmcb-bordeaux.cnrs.fr

Received 24 April 2006, in final form 19 May 2006
Published 19 June 2006
Online at stacks.iop.org/JPhysCM/18/6045

Abstract

The hydrides $CeCoSiH_{1.0}$ and $CeCoGeH_{1.0}$ which crystallize like the parent antiferromagnetic compounds CeCoSi and CeCoGe in the tetragonal CeFeSi-type structure, have been investigated by specific heat and thermoelectric power measurements and ^1H nuclear magnetic resonance (NMR). $CeCoSiH_{1.0}$ is an intermediate valence compound whereas $CeCoGeH_{1.0}$ can be considered as a nearly trivalent cerium compound. This behaviour is corroborated by the occurrence of a slight broadening of the ^1H NMR signal in the sequence $CeCoSiH_{1.0} \rightarrow CeCoGeH_{1.0}$. The band structure calculations performed on these hydrides reveal the existence of strong bonding Ce–H interaction, found to be larger in $CeCoSiH_{1.0}$ than in $CeCoGeH_{1.0}$.

1. Introduction

Recently, we have shown that the ternary compounds based on cerium and crystallizing in the tetragonal CeFeSi-type structure as CeCoSi, CeCoGe or CeMnGe absorb hydrogen [1, 2]. For instance, the hydride $CeCoGeH_{1.0}$ is obtained when CeCoGe ingots are exposed at 393 K for 15–20 h under 2 MPa of hydrogen gas [1]. Moreover, the investigation of this hydride by neutron powder diffraction reveals that (i) it adopts, like the initial ternary germanide CeCoGe, the tetragonal CeFeSi-type structure, and (ii) H (or D) atoms are inserted in the pseudo-tetrahedral interstices [Ce_4] (figure 1) [2] as observed in the crystal structure of the binary hydride CeH_2 [3]. In other words, the structure of $CeCoGeH_{1.0}$ can be described as a stacking along the *c*-axis of two layers formed by [Ce_4Co_4] antiprisms inserting Ge atoms and separated by one layer of [Ce_4] pseudo-tetrahedral units inserting H (or D) atoms. Also, H insertion into these compounds induces an anisotropic expansion of the unit cell parameters:

[3] Author to whom any correspondence should be addressed.

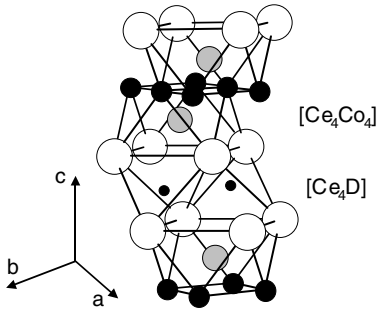

Figure 1. Crystal structure of $CeCoGeD_{1.0}$ (Ce, Co, Ge and D atoms are, respectively, represented by white large, black medium, grey medium and black small circles).

a decreases whereas *c* increases. These structural properties have, as a consequence, (i) the existence of strong Ce–H bonds (*the interatomic distance* d_{Ce-H} *is respectively equal to* 2.391 *and* 2.410 Å in $CeCoSiH_{1.0}$ *and* $CeCoGeH_{1.0}$ [1, 4]; *these values are smaller than that reported 2.417 Å for* CeH_2 [3]) and (ii) a separation between two adjacent blocks of $[Ce_4Co_4]$ antiprisms that is much larger in the hydride than in the parent compound.

Hydrogenation of these ternary compounds strongly modifies their magnetic and electrical properties. For instance, a transition from antiferromagnetic ordering to spin fluctuation behaviour was reported in the sequence CeCoSi $\rightarrow$ $CeCoSiH_{1.0}$ [4]. This result is unusual because hydrogenation generally induces an opposite effect; the increase of the unit cell volume observed by H insertion involves a decrease of the strength of the interaction J_{cf} between 4f (Ce) electrons and conduction electrons, then a stabilization of the magnetic ordering [5]. In order to explain this unusual transition, the electronic and magnetic structures of CeCoSi and $CeCoSiH_{1.0}$ were self-consistently calculated within the local spin density functional (LSDF) theory [4]. Analysis of the electronic structures and of the chemical bonding properties leads us to suggest that the chemical effect of hydrogen prevails over the cell expansion effect which enhances the magnetization in a different way. The demagnetization of cerium at low temperature in $CeCoSiH_{1.0}$ could be associated to the strong Ce–H interaction, which is bonding throughout the conduction band.

We compare here the physical properties of the hydrides $CeCoSiH_{1.0}$ and $CeCoGeH_{1.0}$ for which no long-range magnetic ordering was detected above 1.8 K [1, 4]. We present and discuss their investigation by specific heat, thermoelectric power, ^1H nuclear magnetic resonance (NMR) and band structure calculations using the LSDF theory. For comparison, the antiferromagnetic ordering of CeCoSi and CeCoGe is discussed on the basis of the results obtained using specific heat measurements. Ten years ago, it was reported that these compounds do not show magnetic ordering above 4.2 K [6, 7]. But recent studies claim that CeCoSi and CeCoGe order antiferromagnetically at 8.8 and 5.0 K, respectively [4, 8, 9]. Preliminary results concerning the thermal properties of CeCoSi, CeCoGe and their hydrides were presented recently at the International Conference on Strongly Correlated Electron Systems (*SCES'05, July 26–30 2005, Vienna, Austria*) [10].

2. Experimental procedures

The samples of CeCoSi, CeCoGe and their hydrides were synthesized and characterized by x-ray powder diffraction as described previously [1, 4, 8]. Hydrogenation of CeCoSi and CeCoGe involves an expansion of the unit cell volume of 7.8% and 5.7% respectively.

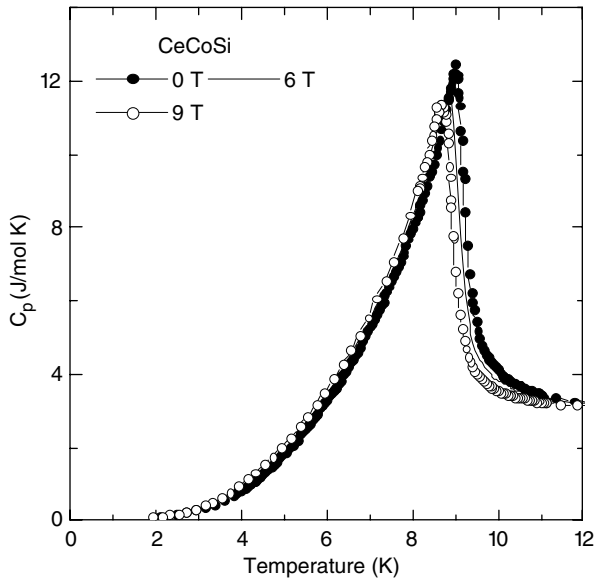

Figure 2. Temperature dependence of the specific heat C_p under several magnetic fields in the ternary silicide CeCoSi.

For specific heat and thermoelectric power measurements, the hydrides were compacted at room temperature (compactness $\cong$ 80%) in order to form a polycrystalline pellet (diameter = 6 mm and thickness = 3 mm) and then heated for two days at 523 K under pressure (5 MPa) of hydrogen. Thermoelectric power investigation was performed on these pellets using a dynamic method. Details of the cell used and measurement methods have been described previously [11]. Heat capacity measurements were performed by a relaxation method with a Quantum Design PPMS system and using a two tau model analysis. Data were taken in the 2–300 K temperature range under applied magnetic fields from 0 to 9 T. For these latter measurements, the samples of hydrides were a plate obtained from the same pellet used for the thermoelectric power measurements.

^{1}H NMR experiments were carried out on $CeCoSiH_{1.0}$, $CeCoGeH_{1.0}$ and $LaCoGeH_{1.0}$ using a solid state Bruker Avance 300 spectrometer (7 T *magnet*), using a 4 mm magic angle spinning (*MAS*) probe. The powder samples were mixed with dry silica in order to facilitate the spinning and to improve the field homogeneity for these materials with metallic conductivity. The spinning speed was 10 kHz, and the recycle time was 2 s. A spin echo sequence (90°-tau-180°) was used with the 90° pulse duration equal to 24 μs and the interpulse delay equal to one rotor period (i.e. 100 μs). The chemical shifts (*ppm*) were referred to external TMS (tetramethylsilane). The spectra were recorded at ambient temperature, although the friction of the drive gas for spinning the rotor at 10 kHz slightly heats the sample to about 300 K.

3. Results and discussion

3.1. Specific heat

As presented in figure 2, the temperature dependence of the specific heat C_p for CeCoSi exhibits a sharp lambda-type magnetic peak centred at 9.0(2) K and a peak value approaching

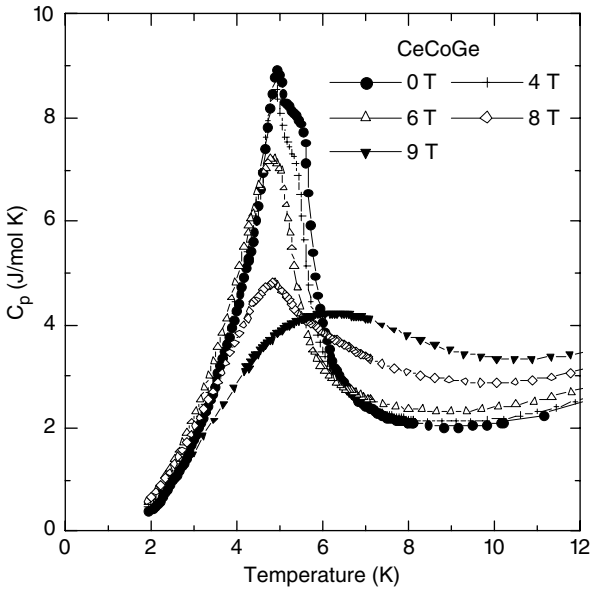

Figure 3. Temperature dependence of the specific heat C_p under several magnetic fields in ternary germanide CeCoGe.

12.5 J mol^{-1} K^{-1} which is smaller than the 15 J mol^{-1} K^{-1} value expected on the basis of mean-field theory. The agreement of transition temperatures T_N measured by magnetic susceptibility ($T_N = 8.8(2)$ K) [4] and heat capacity techniques are clear evidence of antiferromagnetism in CeCoSi. We note also that with increasing magnetic field μ_0H, the lambda-shaped peak continuously diminishes and shifts towards smaller temperatures (*the peak appears at* 8.6(2) K *for* $\mu_0 H = 9$ T) as in conventional antiferromagnet. Valuable information can be obtained from the entropy associated with the antiferromagnetic ordering, which is estimated from the magnetic contribution to the specific heat in the low-temperature range as $C_{\text{p mag}} = C_p - (\gamma + \beta T^2)$ (*between* 12 *and* 25 K, *the fitting* $C_p/T = \gamma + \beta T^2$ *yields to a electronic coefficient* $\gamma = 190$ mJ mol^{-1} K^{-2} *and phonon constant* $\beta = 1.69 \times 10^{-4}$ J mol^{-1} K^{-4}). At T_N, the magnetic entropy reaches 0.48 RLn2, which is substantially reduced from R Ln 2 = 5.76 J mol^{-1} K^{-1}, the value of magnetic entropy expected for a doublet ground state of Ce^{3+}. This reduction suggests the presence of a moderate Kondo effect in this ternary silicide, CeCoSi. This agrees with the small electronic term $\gamma_{LT} = 23$ mJ mol^{-1} K^{-2} deduced from the fitting of the experimental data for $T \leqslant 2.5$ K.

Without applied magnetic field, two anomalies are clearly evidenced from the $C_p = f(T)$ curve for CeCoGe (figure 3): a shoulder appears at $T_{N1} = 5.5(2)$ K which is followed by a peak around $T_{N2} = 4.8(2)$ K [10]. A similar twinned anomaly was confirmed recently by specific heat measurements on a CeCoGe single crystal [9]. This double transition indicates that the antiferromagnetic ordering of CeCoGe is of a more complex form than suggested by magnetization measurement and neutron powder diffraction; these investigations reveal only an antiferromagnetic structure below $T_N = 5.0(2)$ K [8]. We wish to mention here that the temperature dependence of the magnetic susceptibility of this ternary germanide shows a very broad maximum around 5.0(2) K; the broadening could be associated with the existence of two antiferromagnetic transitions. The magnetic entropy at $T_{N1} = 5.5(2)$ K, estimated as previously described above for CeCoSi, reaches 0.64 R Ln 2.

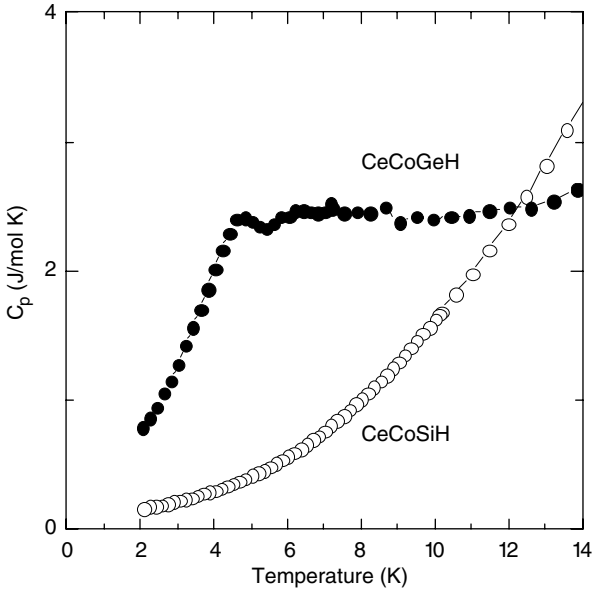

Figure 4. Temperature dependence of the specific heat C_p without magnetic field in the hydrides $CeCoSiH_{1.0}$ and $CeCoGeH_{1.0}$.

The specific heat C_p of CeCoGe was measured at various magnetic fields (figure 3). As for zero field, the $C_p = f(T)$ curve, obtained at 4 T, shows a shoulder around 5.5(2) K and a peak at 4.8(2) K. In contrast, only one peak appears for 6 and 8 T and finally at 9 T a broad bump centred around 6.1(2) K is observed. This latter feature is characteristic of an induced ferromagnetic state resulting from a metamagnetic phase transition evidenced by magnetization measurements on powder [8] or single crystal [9]. Finally, for fields higher than 6 T, some enlargement of C_p occurs above T_{N1}, probably due to Zeeman splitting of the CEF (*crystalline electric field*) ground state.

The investigation of CeCoSi and CeCoGe by specific heat measurements (i) confirms that these compounds exhibit an antiferromagnetic ordering, and (ii) reveals that CeCoGe presents a complex magnetic phase diagram with two transitions evidenced for the first time.

No anomaly can be distinguished from the $C_p = f(T)$ curve observed for $CeCoSiH_{1.0}$ (figure 4), in agreement with the suppression of antiferromagnetic ordering by hydrogenation [4]. The electronic specific heat coefficient, $\gamma = 56$ mJ mol^{-1} K^{-2}, is determined by extrapolation of the $C_p/T = f(T^2)$ curve to zero temperature. It is important to notice that the γ-value is within the range expected for intermediate valence compounds.

In contrast, the $C_p = f(T)$ curve obtained from $CeCoGeH_{1.0}$ (figure 4) exhibits (i) no anomaly around 7.5 K where the magnetic susceptibility goes through a broad maximum [10], and (ii) a small bump close to 4.6 K. Two possible explanations can be proposed for the occurrence of this anomaly: (i) the presence of some amounts of unhydrided germanide CeCoGe (*not detected by x-ray powder diffraction*) showing an antiferromagnetic ordering in this temperature range (*indeed at* 4.6 K, *the magnetic entropy reaches only* $0.27R\ln 2$), or (ii) the existence at low temperatures of some magnetic correlations as in correlated electron systems; it is interesting to note that the C_p value at 2 K is larger for $CeCoGeH_{1.0}$ (0.80 J mol^{-1} K^{-1}) than for CeCoGe (0.47 J mol^{-1} K^{-1}).

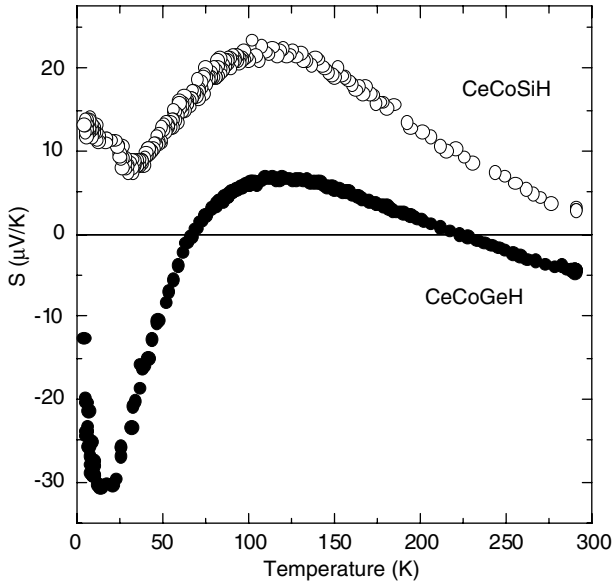

Figure 5. Temperature dependence of the thermoelectric power of the hydrides $CeCoSiH_{1.0}$ and $CeCoGeH_{1.0}$.

3.2. Thermoelectric power

The temperature dependence of the thermoelectric power S of $CeCoSiH_{1.0}$ (figure 5) resembles that observed for $CePd_3$, which is well known as a canonical intermediate valence compound [12, 13]. In the temperature range 4.2–300 K, S is always positive, implying that the dominant carriers are holes, but it presents a minimum at low temperature ($S = 8\ \mu V\ K^{-1}$ near 30–35 K) and a broad peak at high temperature ($S = 22\ \mu V\ K^{-1}$ around 110 K). This behaviour can be qualitatively understood in terms of the Coqblin–Schrieffer model (CSM) which describes the dynamics of conduction electrons due to the exchange and potential scattering on incoherent 4f(Ce) states [13]. This model uses the crystalline electric field (CEF) (Δ *as energy separation between ground and excited levels*) and the number of 4f(Ce) electrons ($n_f \leqslant 1$ *for cerium*). The curve $S = f(T)$ for $CeCoSiH_{1.0}$ is obtained for the CSM model with large CEF splitting and $n_f < 1$ (*strong Kondo temperature* T_K *as in intermediate valence compounds*). This assumption agrees with the existence of a large maximum around 50(5) K for the temperature dependence of the electrical resistivity of $CeCoSiH_{1.0}$ [2]; this behaviour is due to a spin-scattering mechanism in the intermediate valence regime [14].

The $S = f(T)$ curve for the $CeCoGeH_{1.0}$ hydride shows a clearly different behaviour (figure 5). It is mainly characterized by the existence of two extrema: a positive broad maximum of about 7 $\mu V\ K^{-1}$ near 110 K and a pronounced negative $-30\ \mu V\ K^{-1}$ around 16 K. There is also a change in sign close to 66 K. Similar behaviour, characteristic of close to trivalent cerium-based compounds having a low Kondo temperature, has been observed for compounds such as $CeCu_2Si_2$, $CeCu_2Ge_2$, ... [12, 15]. Most of these compounds become superconducting at normal pressure or at very high pressure [16]. The characteristics of the $S = f(T)$ curve for $CeCoGeH_{1.0}$ can be explained using the CSM model [13]: (i) S reaches a zero value at a temperature typically of the order of $3T_K$ (*we estimated* $T_K = 66\ K/3 = 22\ K$ *for this hydride*), and (ii) S goes through a positive maximum at a temperature depending on the CEF (*an increase of* Δ *shifts the temperature of this maximum to higher values*).

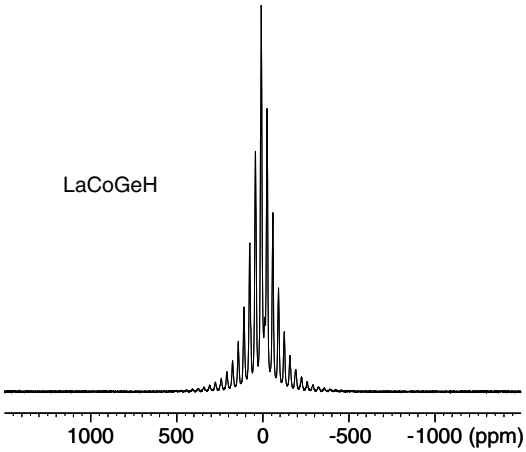

Figure 6. ^{1}H MAS NMR signal for $LaCoGeH_{1.0}$ (Hahn echo, 10 kHz spinning). The lines other than the most intense one are spinning sidebands.

The comparison of the $S = f(T)$ curves for $CeCoSiH_{1.0}$ and $CeCoGeH_{1.0}$ evidences that the electronic state of cerium is different in these two hydrides. Moreover, the changes of the $S = f(T)$ curve from $CeCoGeH_{1.0}$ to $CeCoSiH_{1.0}$ can be compared to those reported by Link *et al* [15] which have applied isostatic pressure on the ternary germanide $CeCu_2Ge_2$. Without pressure, S for the latter compound exhibits at low temperature ($\widetilde{=}$20 K) a negative peak followed by a broad positive contribution (80–100 K) with increasing temperature. In contrast, under a pressure of 16.5 GPa, S is always positive, showing a shoulder near 20–40 K and a strong positive peak around 150 K with increasing temperature. The transition between these two behaviours is explained by the sequence close to trivalent cerium $\rightarrow$ intermediate valence cerium induced by the pressure. This comparison is in agreement with an increase of the Kondo temperature in the sequence $CeCoGeH_{1.0} \rightarrow CeCoSiH_{1.0}$ as detected by magnetization measurements [1, 4].

3.3. ^{1}H NMR

Figure 6 shows the ^{1}H MAS NMR spectrum of the metallic $LaCoGeH_{1.0}$ hydride which does not contain 4f electrons. The main sources of dipolar interaction expected in such a case are homonuclear dipolar interaction, which is classically rather strong in solids, and ^{1}H–^{139}La heteronuclear dipolar interaction, considering four nearest La neighbours with a nearly 100% abundance and a gyromagnetic ratio about 15% that of a proton. MAS nevertheless strongly decreases this interaction and leads to a separation into relatively sharp spinning sidebands. The position of the isotropic signal is 8.7 ppm, showing no significant Knight shift contribution, despite the metallic-type conductivity exhibited by this compound. This shows that the electron of hydrogen is transferred to the band structure of the compound and that the s orbital of proton does not participate significantly to the DOS at the Fermi level (*where it would experience the Pauli paramagnetism of the conducting electrons leading to a stronger Knight shift of the NMR line*). We note also no influence of cobalt on the ^{1}H signal, confirming that this element carries no magnetic moment.

As shown in figure 7, the ^{1}H MAS NMR spectrum of the $CeCoGeH_{1.0}$ hydride is not even separated into spinning sidebands, showing a very strong dipolar interaction although Ce does

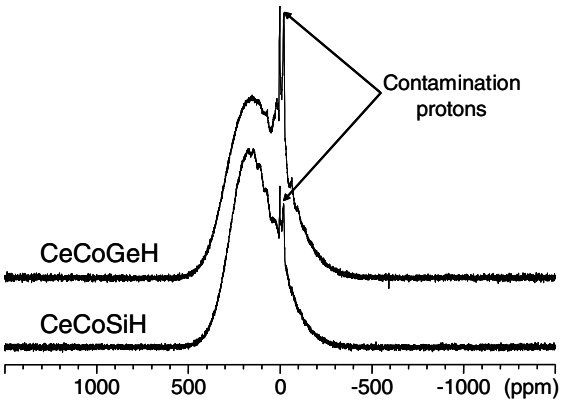

Figure 7. ^{1}H MAS NMR signal for $CeCoSiH_{1.0}$ and $CeCoGeH_{1.0}$ (Hahn echo, 10 kHz spinning).

not carry a nuclear spin; this is therefore due to the localized electron spins present on the Ce^{3+} ions' 4f orbitals. Indeed, the gyromagnetic ratio of the electron is 700 times as large as that of the ^{1}H nucleus, leading to extremely strong dipolar interactions which can hardly be averaged out by MAS. Besides, the position of the signal is strongly shifted to about 150 ppm, which suggests a Fermi contact interaction (*transfer of some density of electron spin from Ce to proton via orbital overlap*), again in good agreement with the band structure calculations (*see below*). In addition to the signal discussed above, narrow signals are also observed around 0 ppm, due to traces of protons in the NMR probe and/or at the surface of the sample. Such signals can also be observed by close observation of the $LaCoGeH_{1.0}$ spectrum (figure 6) with a smaller apparent intensity due to the shape of the main signal.

As shown in figure 7, the ^{1}H MAS NMR signal of $CeCoSiH_{1.0}$ is quite similar to that of $CeCoGeH_{1.0}$, except for a slightly better separation into spinning sidebands and for a very slightly smaller overall width. This suggests a slightly weaker dipolar interaction from the electron spins on cerium, in good agreement with the investigation of its magnetic and transport properties which suggest an intermediate valence state of cerium in $CeCoSiH_{1.0}$. The position of the NMR line is very similar in the two compounds; the stronger Ce–H bonding shown by the calculations in the case of $CeCoSiH_{1.0}$ therefore seems to lead to a similar ^{1}H Fermi contact shift despite the smaller electron spin density on cerium compared with the case of $CeCoGeH_{1.0}$.

3.4. Band structure calculations

Within the density functional theory (DFT) [17, 18] in its local spin density approximation of the effects of exchange and correlation [19, 20], we have used the all-electron scalar relativistic augmented spherical wave (ASW) method [21–23]. All valence electrons, including 4f(Ce), were treated as band states. In the minimal ASW basis set, we chose the outermost shells to represent the valence states and the matrix elements were constructed using partial waves up to $l_{max} + 1 = 4$ for Ce, $l_{max} + 1 = 3$ for Co and $l_{max} + 1 = 2$ for Ge.

In so far as both hydrides are spin fluctuation systems [1, 4] in the ground state our analyses assume non-magnetic configurations (*non-spin-polarized: NSP*), meaning that spin degeneracy was enforced for all species. Such a configuration is however not relevant to a paramagnet, which would only be simulated by a huge supercell, entering random spin orientation over the different magnetic sites. Here we report on the density of states (DOS) and chemical

bonding features. These are inferred from the ECOV (*covalent bond energy*) criterion [24] which makes use of both overlap (S_{ij}) and Hamiltonian (H_{ij}) populations to account for the chemical interactions. Bonding and antibonding interactions are translated by negative and positive ECOV magnitudes.

Accurate calculations using experimental data of the $CeCoGeH_{1.0}$ hydride [1, 2] were carried out in the same conditions as in the previous work devoted to CeCoSi and $CeCoSiH_{1.0}$ [4].

We point out that the same trends observed in the ternary silicide systems apply here: this stands namely for the spin fluctuation behaviour observed upon hydriding, which is translated in the computation results by the absence of ordered moments in the ground state when spin polarization was allowed for. The Fermi levels of both systems are different: $E_F(CeCoGeH_{1.0}) = 0.5835$ Ryd and $E_F(CeCoSiH_{1.0}) = 0.5908$ Ryd. We focus here on the comparative analyses of both hydride systems by discussing the site projected DOS and the chemical bonding.

For computations carried out in the same conditions of convergence precision as in [4], a relevant feature is the redistribution of the $4f^2$ valence electrons over 4f and 5d states due to the quantum mixing with the other ligand valence basis set states. Such itinerant states are actually responsible for the major part of the chemical bonding within the valence band. This is in relation to the intermediate valence state of Ce within the two systems as theoretically proposed by Long in cerium-based intermetallics [25].

3.4.1. Density of states (DOS) and chemical bonding (ECOV). In so far as the plots show similar features between the two systems [4], we only present here the DOS and ECOV results for $CeCoGeH_{1.0}$ in figure 8. The Fermi level (E_F) is taken as zero energy.

DOS. Looking firstly at the density of states (figure 8(a)), the cerium DOSs are seen to prevail through the large peak around E_F mainly due to 4f(Ce) states. There is a non-negligible contribution from Ce itinerant states below E_F which ensure the chemical bonding through hybridization with the other metallic species (figure 8(b)) as well as with H, as is shown in figure 8(c). Due to the large filling of their d-states, the cobalt DOSs are found completely within the valence band (VB). They show similar shape at the low energy part of the VB, i.e. [−6, −2 eV] which is a feature pointing to a mixing between Co, Si and Ce (see the next paragraph). Hydrogen partial DOSs were artificially multiplied by 5 in order to clearly exhibit their contribution within the VB. They can be seen to have a similar skyline to other states within the VB, which is a token of the quantum mixing with the metal species valence states as is shown hereafter.

ECOV. Just like in $CeCoSiH_{1.0}$ [4], the ECOV curves for Ce–Co, Ce–Ge and Co–Ge pair interactions (figure 8(b)) show that Co–Ge is prevailing with respect to Ce–Co than to Ce–Ge which is weakest. For the metallic pair interactions the major part of the VB is bonding with antibonding ECOV starting to appear in the neighbourhood of E_F, especially for Co–Ge.

Figure 8(c) gives the metal–hydrogen contribution to the bonding. The (y) scale is of much smaller magnitude than in figure 8(b) which shows that the metal–metal and metal–p-element interaction is relatively stronger. Here the prevailing interaction is for the Ce–H interaction which is bonding throughout the whole energy range, from −4 eV up into the conduction band. In contrast, there is a strong antibonding contribution for Co–H around −2 eV due to the larger filling of the cobalt d-states. Both Ce–H and Co–H interactions show similar shapes around −3 and −1 eV on both sides of the antibonding region.

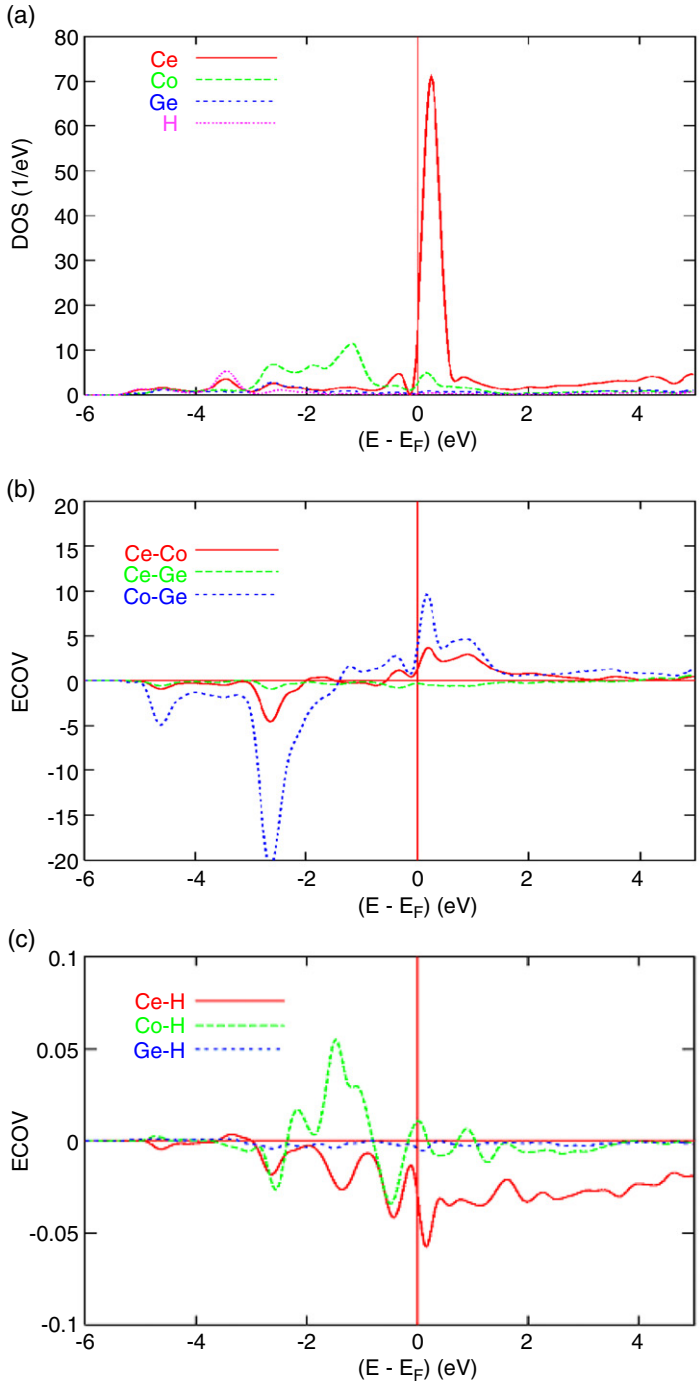

Figure 8. NSP $CeCoGeH_{1.0}$ plots: (a) site projected DOS, (b) and (c) chemical bonding using the ECOV criterion respectively for metal–metal and metal–H.

(This figure is in colour only in the electronic version)

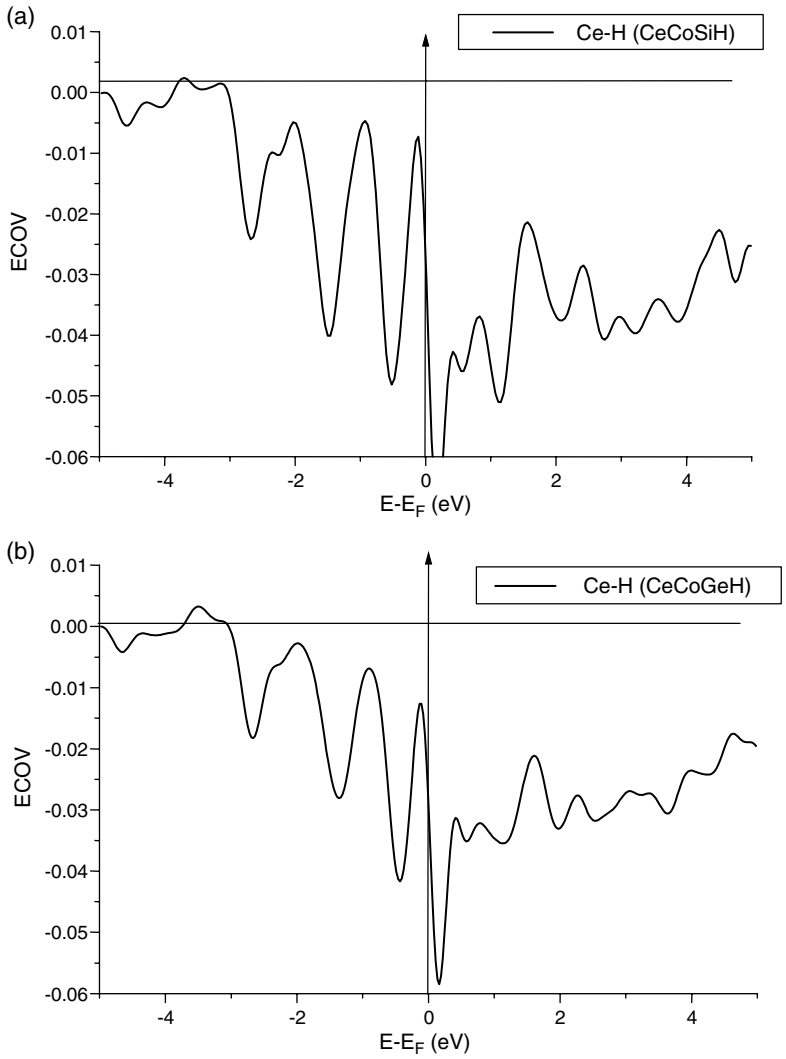

Figure 9. Comparative plots of Ce–H ECOV: within (a) $CeCoSiH_{1.0}$ and (b) $CeCoGeH_{1.0}$ systems. The former integrates to ∼10% more area than the latter.

For the sake of better understanding the qualitative differences underlying the $CeCoSiH_{1.0}$ versus $CeCoGeH_{1.0}$ systems, we show in figure 9 comparative plots of the Ce–H interaction within the two hydrides at the same scale for ECOV (y) and energy (x) axes. As can be observed from the relative intensities, the Ce–H ($CeCoSiH_{1.0}$) interaction is found larger than the Ce–H ($CeCoGeH_{1.0}$) one and the integration of both curves points to a ratio of ∼1.075, i.e., with a 10% larger Ce–H bonding within $CeCoSiH_{1.0}$. This result is related to the experimental results of the larger mixed valence character of cerium within $CeCoSiH_{1.0}$ than within $CeCoGeH_{1.0}$, as can be inferred from the above results.

4. Conclusion

Specific heat measurements performed on CeCoSi, CeCoGe and their hydrides clearly indicate the absence of magnetic ordering for $CeCoSiH_{1.0}$ but reveal the occurrence of magnetic

correlations below 4.6 K for $CeCoGeH_{1.0}$. The thermal dependence of the thermoelectric power of $CeCoSiH_{1.0}$ agrees with its intermediate valence compound behaviour whereas that concerning $CeCoGeH_{1.0}$ suggests that cerium is nearly trivalent in this hydride. These two different electronic states of the cerium in $CeCoSiH_{1.0}$ and $CeCoGeH_{1.0}$ are evidenced by ^1H NMR; the ^1H MAS NMR signal is slightly narrower for $CeCoSiH_{1.0}$, indicating slightly weaker dipolar interaction from the electron spins on cerium (*intermediate valence state*). Finally, all the results deduced from the hydrogenation of CeCoSi and CeCoGe, which destroys their antiferromagnetic ordering, can be explained on the basis of the band structure calculations. The existence of strong bonding Ce–H interaction, found to be larger in $CeCoSiH_{1.0}$ than in $CeCoGeH_{1.0}$, plays an important role on the physical properties of these hydrides $CeCoSiH_{1.0}$ and $CeCoGeH_{1.0}$.

Acknowledgments

Stimulating discussions concerning the thermoelectric properties of the hydrides with Dr B Coqblin (Orsay, France) are gratefully acknowledged. We wish to thank the European Science Foundation (ECOM-COST action P16) for financial support. We acknowledge calculation facilities provided by the 'M3PEC-Mésocentre Régional' main frame supercomputers of the University Bordeaux 1 financed by the University, the 'Conseil Régional d'Aquitaine' and the French Ministry of Research and Technology.

References

[1] Chevalier B, Gaudin E, Weill F and Bobet J-L 2004 *Intermetallics* **12** 437
[2] Chevalier B, Pasturel M, Bobet J-L and Isnard O 2005 *Solid State Commun.* **134** 529
[3] Holley C E Jr, Mulford R N R, Ellinger F H and Koehler W C 1955 *J. Phys. Chem.* **59** 1226
[4] Chevalier B and Matar S F 2004 *Phys. Rev.* B **70** 174408
[5] Chevalier B, Pasturel M, Bobet J-L, Decourt R, Etourneau J, Isnard O, Sanchez Marcos J and Rodriguez Fernandez J 2004 *J. Alloys Compounds* **383** 4
[6] Welter R, Venturini G, Ressouche E and Malaman B 1994 *J. Alloys Compounds* **210** 279
[7] Welter R, Venturini G, Malaman B and Ressouche E 1993 *J. Alloys Compounds* **201** 191
[8] Chevalier B and Malaman B 2004 *Solid State Commun.* **130** 711
[9] Vejpravova J, Prokleska J, Janousova B, Andreev A V and Sechovsky V 2006 *Physica* B at press
[10] Chevalier B, Matar S F, Sanchez Marcos J and Rodriguez Fernandez J 2006 *Physica* B at press
[11] Dordor P, Marquestaut E and Villeneuve G 1980 *Rev. Phys. Appl.* **15** 1607
[12] Jaccard D, Flouquet J and Sierro J 1985 *J. Appl. Phys.* **57** 3084
[13] Zlatic V, Horvatic B, Milat I, Coqblin B, Czycholl G and Grenzebach C 2003 *Phys. Rev.* B **68** 104432
[14] Cornut B and Coqblin B 1972 *Phys. Rev.* B **5** 4541
[15] Link P, Jaccard D and Lejay P 1996 *Physica* B **225** 207
[16] Jaccard D, Wilhelm H, Alami-Yadri K, Vargoz E and Lejay P 1999 *Physica* B **259–261** 1
[17] Kohn W and Sham L J 1965 *Phys. Rev.* A **140** 1133
[18] Hohenberg P and Kohn W 1964 *Phys. Rev.* B **136** 864
[19] von Barth J and Hedin D 1972 *J. Phys. C: Solid State Phys.* **5** 1629
[20] Perdew J and Zunger A 1981 *Phys. Rev.* B **23** 5048
[21] Williams A R, Kübler J and Gelatt C D Jr 1979 *Phys. Rev.* B **19** 6094
[22] Eyert V 2000 *Int. J. Quantum Chem.* **77** 1007
[23] Kölling D D and Harmon B N 1977 *J. Phys. C: Solid State Phys.* **10** 3107
[24] Bester G and Fähnle M 2001 *J. Phys.: Condens. Matter* **13** 11541
Bester G and Fähnle M 2001 *J. Phys.: Condens. Matter* **13** 11551
[25] Long M W 1989 *J. Phys.: Condens. Matter* **1** 10321